# Usage of synchrotron radiation for analyzing texture inhomogeneity in zirconium-based alloy tubes

***M. G. Isaenkova****, Professor, Doctor of Physical and Mathematical Sciences[1], e-mail: MGIsaenkova@mephi.ru*
***O. A. Krymskaya***, *Associate Professor, Candidate of Physical and Mathematical Sciences[1], e-mail: OAKrymskaya@mephi.ru*
***V. A. Rogovskiy***, *Engineer[1], e-mail: victor_rsn@bk.ru*
***I. V. Kozlov***, *Associate Professor, Candidate of Technical Sciences[1], e-mail: ilya_mephist@mail.ru*
***V. A. Fesenko***, *Lead Engineer[1], e-mail: fesenko.vlad@mail.ru*

[1]*National Research Nuclear University "MEPhI", Moscow, Russia.*

This paper presents the results of using synchrotron radiation to study the circumferential and layer-by-layer inhomogeneity of zirconium alloy tubes. Reducing the size of the initial synchrotron beam to 200×200 μm allows us to analyze the layer-by-layer inhomogeneity of tubes with a wall thickness of 600 μm and above. Based on the results of the analysis of the circumferential inhomogeneity of the cladding tubes and guide channels for the integral texture *f*-parameters, the error value was 0.04, which is twice as high as the error when using the standard *X*-ray method. The maximum error in integral texture *f*-parameters is achieved for recrystallized samples, i.e. when the number of grains from which the diffraction pattern is formed decreases. The division of Debye rings into individual reflections also leads to a reduction of the statistical significance of the data obtained and an increase in the error in processing the diffraction patterns. Layer-by-layer analysis of the studied cold-rolled and annealed tubes made it possible to identify the features of plastic deformation of the tubes.

**Key words:** syncrotron radiation, zirconium, crystallographyc texture, inhomogeneity, cold rolling, *X*-ray analysis, heat treatment, structure.

***DOI:*** 10.17580/nfm.2025.02.06

## Introduction

In zirconium-based alloy tubes, as in any other metal products with a developed crystallographic texture, a certain hierarchy of structural and textural inhomogeneities exists, the levels of which differ in the volume (or area) of the manifestation areas [1]. That is, a comparison of textures within areas of a certain size allows characterizing the textural inhomogeneity at the corresponding scale level using the differences identified. Thus, the textural inhomogeneity of the material reflects the inhomogeneity of the plastic deformation in it [2, 3], and also determines the properties associated with the existing gradient of structure and texture.

In reality, plastic deformation always develops inhomogeneity – only the dimensions of inhomogeneous regions varies. In particular, within the same grain, plastic deformation of the boundary and internal areas proceeds differently, with the participation of a different number of slip systems, which leads to different lattice rotations and additional grain fragmentation. Neighbouring grains with different crystallographic orientations are deformed differently, since shear stresses in potential slip and twinning systems are determined by the orientation of the systems relative to the loading axes. These variants of non-uniform deformation development always occur, and, considering them in relation to ordinary polycrystalline materials, it is appropriate to speak of structural inhomogeneity at the micro-level [2].

At the next structural level, corresponding to a statistically significant set of grains, for which the term "texture" is applicable (it is called the meso-level), the inhomogeneity of deformation development generates structural heterogeneities of a statistical nature and, first of all, local heterogeneities of texture. At the macro-level, the inhomogeneity of the plastic deformation process is caused by differences in the conditions of loading and flow of the material in different areas. As a result (in particular, in a tube), layer-by-layer inhomogeneity of texture develops naturally during rolling. In the same tube, during straightening, zones of additional deformation work hardening appear, where, during subsequent heat treatment, preferential recrystallization occurs [1–6].

In the study [2] during the research of the textural inhomogeneity of cladding tubes, various approaches were used:

1) *X*-ray texture shooting of various sections of the tube under study, allowing, in particular, to identify its layer-by-layer and circumferential textural inhomogeneity;

2) comparison of the texture of individual tubes obtained from the same alloy according to the same process scheme allows to identify inhomogeneity caused by incomplete reproducibility of the plastic flow processes and texture formation during the transition from tube to tube or during movement along its length;

*Correspondence author.

3) assessment of textural inhomogeneity by the asymmetry of the DPF, indicating the inhomogeneity of the deformation development within one sample with an area of several square millimetres with a reflective layer thickness of several microns.

If the loading scheme of the tube material during its manufacture is symmetrical with respect to the *L*-*R*-plane containing the axial (*L*) and radial (*R*) directions, the texture direct pole figures (DPFs), according to the Curie principle [7], should have at least the same symmetry, and, therefore, the left and right parts of the DPF should be mutually identical. Indeed, under symmetric loading there is no reason for a preferred orientation of the basal axes in the left or right parts of the DPF, so that the crystallographically equivalent left and right texture components (e.g., (0001) + 30–50° *R*-*T*<10$\bar{1}$0> and (0001) – 30–50° *R*-*T*<10$\bar{1}$0>) should be equal in intensity. However, a necessary condition for such equality is the presence in the reflecting volume of a statistically sufficiently large number of grains in the absence of a long-range correlation between their orientations.

It has been shown previously [2] that the presence of layer-by-layer inhomogeneity of the crystallographic texture in zirconium tubes operated in extreme conditions of a nuclear reactor core and subject to cyclic heating and cooling during power maneuvering the reactor power can cause the development of high stresses that promote the reorientation of the hydride phase from the tangential direction to the radial direction and promote subsequent embrittlement of the tube material.

Previously used diffractometric methods for measuring crystallographic texture were related to samples composed of 5–7 tube segments, characterized by a deviation of the studied surface from the radial direction by angles from 8 to 12°. In the case of using synchrotron radiation, it is possible to reduce this deviation to 2–3° depending on the tube diameter, since the dimensions of the synchrotron beam are 200×200 μm. This helps to increase the accuracy of the measurements.

Previously developed methods for calculating [8–10] the grain orientation distribution function (ODF) and DPFs based on the results of processing Debye rings obtained by the transmission method of foils 120–150 μm thick make it possible to increase the accuracy of measuring the layer-by-layer change in the texture of cladding tubes and guide channels.

This work is devoted to the description of the method for using synchrotron radiation to analyse the circumferential and layer-by-layer texture inhomogeneity of cladding tubes made of Zr – 1%Nb – (Fe, O) alloy and guide channels made of Zr – 1%Nb – 1.2%Sn – (Fe, O) alloy.

**Materials and methods of tubes inhomogeneity research**

The analysis of the crystallographic texture along the circumference and wall thickness of the tubes was carried out on deformed and annealed samples of cladding tubes made of Zr – 1.0Nb – (0.06Fe – 0.08O) alloy, wt.% (hereinafter referred to as alloy No. 1) and guide channels made of Zr – 1%Nb – 1.2%Sn – (0.35Fe – 0.08O) alloy, wt.% (hereinafter referred to as alloy No. 2). According to the results of [8–10] using synchrotron data, it was established that the main phase of the studied alloys is a solid solution of alloying elements in the HCP structure of α-Zr. Alloy No. 2 is characterized by the presence of an additional stable Laves phase Zr(Nb, Fe)$_2$, which retains its structure both in the deformed state and during subsequent annealing in the temperature range of 480–640 °C. In the deformed alloy No. 1 additional phases are solid solutions in the BCC (body centred cubic) structure with different elemental composition (β-Nb, β-Zr) and the Laves phase. The amounts of additional phases do not exceed 2–3 wt.%. It has been shown [9, 10], that the rolling texture of α-Zr for medium-thickness wall layers of the material corresponds to that measured earlier for surface layers using *X*-ray analysis, namely, the following rolling texture is observed in the volume of the rolled material: (0001) ± 30–45° *R*-*T*<10$\bar{1}$0>, where *R* and *T* are the radial and tangential directions, respectively. As a recrystallization result of α-Zr phase, the deformation texture is replaced by the recrystallization texture (0001) ± 30–45° *R*-*T*<11$\bar{2}$0>, which is caused by the absorption of the deformed matrix by recrystallized grains misoriented relative to the original grains by a rotation of 30° around the basal axes. Based on the results of the synchrotron study dependences of the change in the ratio of the pole densities of the axes <11$\bar{2}$0> and <10$\bar{1}$0>, oriented along the rolling direction of the tubes, were obtained, which characterize the completeness of the recrystallization at different annealing temperatures during 1–6 hours [2, 6].

The obtained data were used in the analysis of the layer-by-layer inhomogeneity of the crystallographic texture of the tubes under consideration. The study of the layer-by-layer inhomogeneity of zirconium tubes was carried out on samples in the form of rings with axial thickness 120–150 μm, cut from cladding tubes made of alloy No. 1 and guide channels made of alloy No. 2. The description of the studied samples is presented in **Table 1**. Additionally, **Table 1** presents the results of the studying the tubes structure and texture, previously obtained using traditional *X*-ray diffraction research methods.

In the case of using the standard geometry of texture recording on an *X*-ray diffractometer, it is necessary to prepare a flat composite sample, which is a section of a tube, the middle part of which is perpendicular to the radial direction [9]. However, during such recording, in various areas of the sample, the normal direction to the surface of the section under study deviates from the *R*-direction by an angle of up to 12°. In this case, a blurring of the DPFs in the *R*-*T*-section of the tube is noted, as was shown in [9]. This prevents obtaining correct information about the crystallographic texture of various sections of the tubes.

In this study, an algorithm for studying the crystallographic texture of materials using Debye rings obtained with synchrotron *X*-ray radiation during shooting of foils

Table 1
**Description of the studied samples**

| Sample No. | Alloy | Tube diameter, mm | | The last treatment | $a$, Å | $c$, Å | $c/a$ | $f$-parameters | | |
|---|---|---|---|---|---|---|---|---|---|---|
| | | Inner | Outer | | | | | $f_R$ | $f_T$ | $f_L$ |
| 1.1 | Zr – 1%Nb – (Fe, O) (No. 1) | 9.50 | 8.33 | Cold-Rolled | 3.2424 | 5.1394 | 1.5851 | 0.60 | 0.35 | 0.05 |
| 1.2 | | | | 480 °C – 3 h | 3.2344 | 5.1499 | 1.5922 | 0.59 | 0.35 | 0.06 |
| 1.3 | | | | 580 °C – 3 h | 3.2316 | 5.1522 | 1.5943 | 0.58 | 0.35 | 0.07 |
| 1.4 | | | | 600 °C – 3 h | 3.2317 | 5.1513 | 1.5940 | 0.60 | 0.34 | 0.06 |
| 2.1 | Zr – 1%Nb – 1.2%Sn – (Fe, O) (No. 2) | 12,9 | 10,9 | Cold-Rolled | 3.2381 | 5.1433 | 1.5884 | 0.58 | 0.36 | 0.06 |
| 2.2 | | | | 480 °C – 3 h | 3.2312 | 5.1481 | 1.5932 | 0.61 | 0.34 | 0.05 |
| 2.3 | | | | 580 °C – 3 h | 3.2300 | 5.1522 | 1.5951 | 0.52 | 0.42 | 0.06 |
| 2.4 | | | | 600 °C – 3 h | 3.2302 | 5.1520 | 1.5949 | 0.56 | 0.38 | 0.06 |

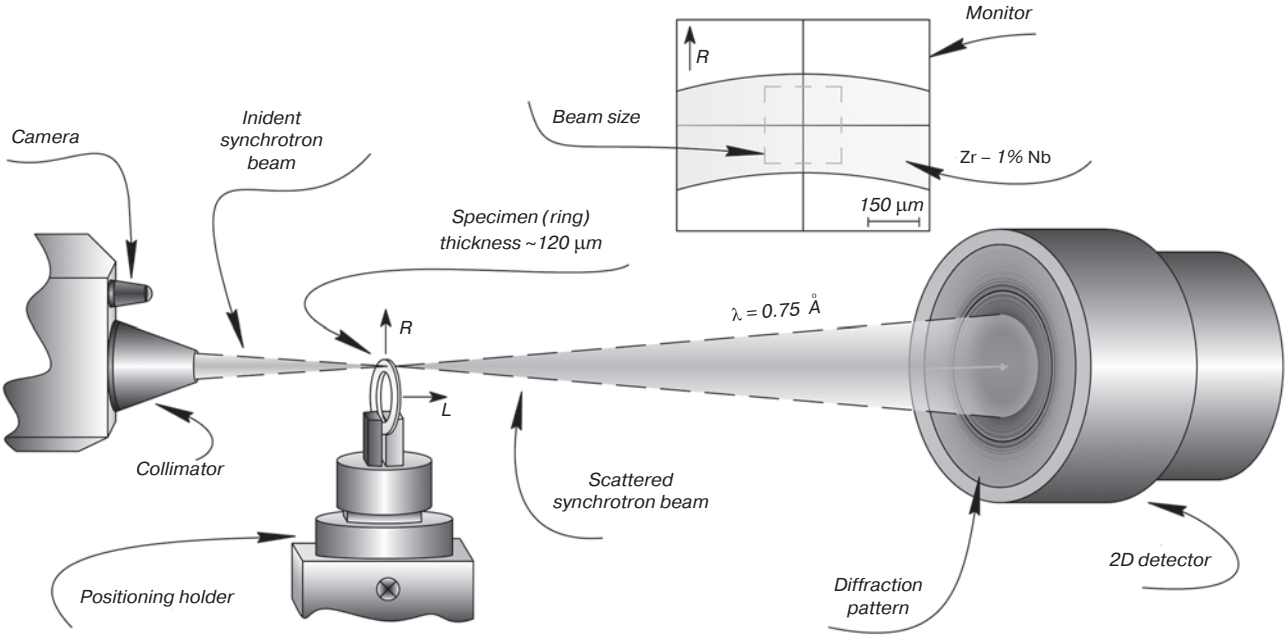


**Fig. 1.** Geometry of diffraction pattern shooting using a synchrotron beam at the BELOK/RSA KISI-Kurchatov station

up to 150 μm thick is optimized. The sample shooting method is shown in **Fig. 1**. The ODFs and complete DPFs for the α-phase and for phases present in the material in small quantities are constructed for deformed and annealed zirconium alloys.

**Fig. 2** schematically shows the investigated areas of the foils in the form of rings, the plane of which is perpendicular to the axis of the analyzed tubes. The analysis of the circumferential and layer-by-layer inhomogeneity of the tubes was carried out using synchrotron radiation, for which the projection of the primary beam of a square cross-section has dimensions of 200 × 200 μm. Debye rings were recorded for different sections of the tubes along the circumference **(Fig. 2, *a*)** and along the wall thickness **(Fig. 2, *b*)**.

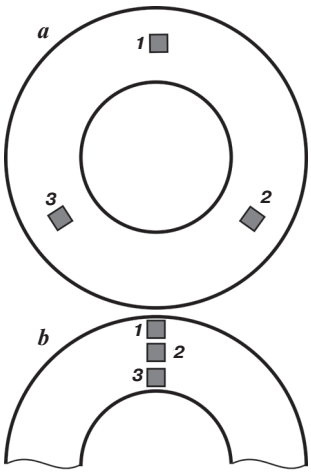


**Fig. 2.** Scheme of the study of circumferential (*a*) and layer-by-layer (*b*) inhomogeneity of tubes

The following labeling of the samples was used: the first digit in the label corresponds to the alloy number, the second — to the structural state: 1 – cold-rolled alloy, 2 – annealed at 480 °C for 3 hours; 3 – annealed at 580 °C for 3 hours; 4 – annealed at 600 °C for 3 hours; the third digit will be used to designate different sections of the tube along the circumference **(Fig. 2, *a*)** or the studied layer along the wall thickness, in which the counting starts from the outer surface of the tube **(Fig. 2, *b*)**.

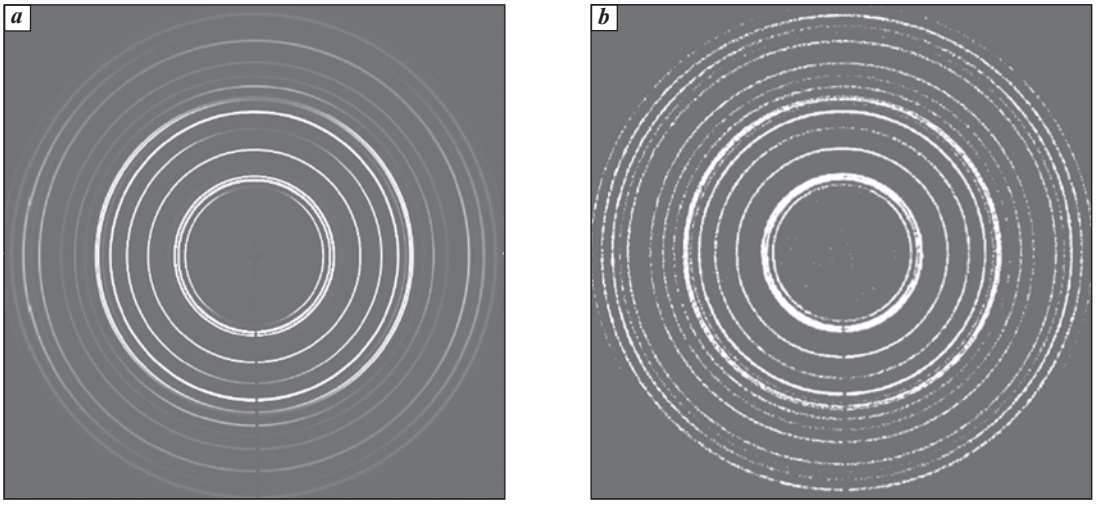


**Fig. 3.** Debye rings obtained by shooting the middle layers along the thickness of cold-rolled (*a*) and annealed at 580 °C (*b*) tubes made of alloy No. 1

### Sequence of processing of obtained synchrotron images

First of all, a shooting of the $LaB_6$ standard is carried out, according to which the shooting geometry and the wavelength of synchrotron radiation are specified. The obtained shooting parameters are then used to process the Debye rings obtained for the all studied samples. The error in reproducing the experimental spectrum of the $LaB_6$ standard is 7–10%.

**Fig. 3** shows examples of Debye rings for the alloy No. 1 in the deformed (*a*) and annealed (580 °C) (*b*) states. The presented images show, how continuous rings in the deformed sample are transformed into rings consisting of individual reflections.

**Fig. 4** shows the diffraction pattern of deformed alloys No. 1, calculated from Debye rings **(Fig. 3, *a*)** using the MAUD software [11–19]. **Table 2** shows the results of calculating the volume fractions and structural characteristics of three phases (Laves phase, α- and β-zirconium) for both alloys in different states.

The complete DPFs calculated in the MAUD software for α-zirconium represent the $DPF_L$ for the tube cross-section perpendicular to the axial direction *L*. The obtained $DPF_L$ are rotated relative to the external directions in order to obtain the $DPF_R$ for the R-section and calculated the integral Kearns texture parameters (*f*-parameters) that determine the anisotropy of the physical and mechanical properties of the material [23]. The DPFs rotation was performed in the freely distributed MTEX software [24]. Thus, the ODFs were constructed based on the Debye rings and the complete DPFs for the *R*-section (18 reflections) were calculated **(Fig. 5)**.

The obtained results of phase analysis indicate that alloy No. 1 consists of three phases: α-zirconium, Laves phase and β-zirconium, and alloy No. 2 consists of two phases: α-zirconium and Laves phase. The BCC phase could not be detected in alloy No. 2.

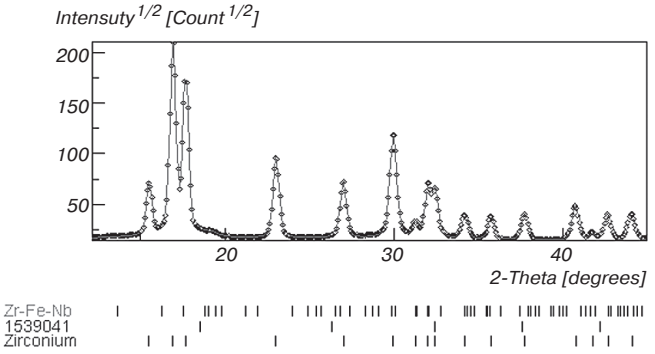


**Fig. 4.** Diffraction pattern calculated from Debye rings. Black dots correspond to experimental intensities calculated from Debye rings; the solid curve is calculated for three phases: α-zirconium; Laves phase; β-phase of alloy No. 1

### Results of circumferential inhomogeneity of the studied tubes

The circumferential inhomogeneity studies were carried out on deformed and annealed at a temperature of 580 °C for 3 hours samples of both alloys No. 1 and No. 2: 1.1 and 1.3; 2.1 and 2.3, respectively. The middle layers along the wall thickness of the tubes were studied. When calculating the error associated with circumferential inhomogeneity and given in **Table 2**, the results obtained from the analysis of circumferential inhomogeneity of deformed and recrystallized tubes were taken into account, as well as the data for the middle layers of the samples obtained from the analysis of the layer-by-layer tubes inhomogeneity.

The **Table 2** shows the error of processing Debye rings, the lattice parameters, the coherent block size *D* and the microdistortions $\Delta d/d$ of the α-phase. Considering that the share of additional phases does not exceed 3% and, moreover, is determined with a high error, their structural characteristics are not given.

The error in processing synchrotron data depends on the error in processing the reference data, as well as on

the quality and statistical significance of the results obtained. The fragmentation of continuous Debye rings observed for a deformed material into individual spots formed in the recrystallized state as a result of the growth and decrease in the number of reflecting grains (see **Fig. 3**) leads to a significant increase in the error in processing the primary pattern reconstructed from the Debye rings (see **Table 2**). However, despite the high error in data processing, a natural change in the lattice parameters of the main α-zirconium phase is observed **(Table 2)** as a result of annealing the deformed alloys, which corresponds to the changes obtained earlier for zirconium alloys [2, 12, 13]. As a result of annealing tubes made of different alloys at a temperature of 580 °C for 3 hours, a decrease in the lattice parameter "*a*" and an increase in the parameter "*c*" are observed. It was noted earlier that the parameter "*a*" is more sensitive to the degree of deformation of the alloy, and alloys No. 1 and No. 2 have different values of the specified parameter "*a*" [10]. In this case, differences in the parameters "*a*" for annealed alloys are also noted (compare results in **Tables 1, 2**). If the error in measuring the lattice parameters by traditional *X*-ray methods is about 0.0001 Å, then it follows from **Table 2** that the circumferential inhomogeneity of determining the lattice parameters significantly exceeds the instrumental error of measuring. This may be due to the inhomogeneity of deformation across the thickness of the tube wall and the spread of grain microdistortion $\Delta d/d$ in deformed tubes.

In **Table 2** is also presented the spread range in determining of integral texture *f*-parameters. According to the

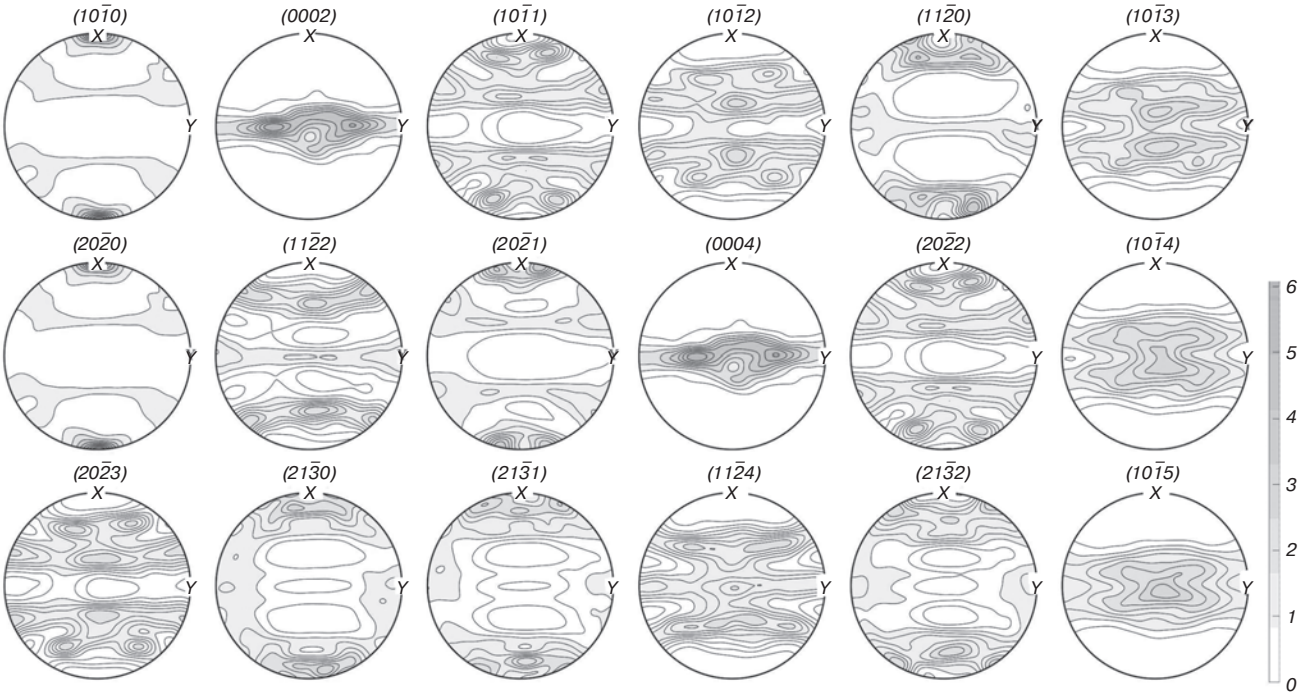


**Fig. 5.** The complete $DPF_R$ of α-zirconium cold-rolled alloy No. 1 (18 reflections)

Table 2

**Structural characteristics of the average cross-section by wall thickness of tubes made of alloys No. 1 and No. 2**

| Sample No. | Processing error, % | Phase ratio $x_\alpha/x_{Laves}/x_\beta$, vol. % | Lattice parameters | | *D*, Å | $\Delta d/d$, % | *f*-parameters | | |
|---|---|---|---|---|---|---|---|---|---|
| | | | *a*, Å | *c*, Å | | | *R* | *T* | *L* |
| 1.1 | 13.23 ± 2.54 | 98.90 ± 0.32<br>0.41 + 0.18<br>0.69 + 0.47 | 3.2391 ± 0.0016 | 5.1420 ± 0.0035 | 545 ± 63 | 0.34 ± 0.02 | 0.59 ± 0.01 | 0.34 ± 0.01 | 0.06 ± 0.01 |
| 1.3 | 28.4 ± 2.49 | 99.00 ± 0.44<br>0.85 + 0.42<br>0.15 ± 0.14 | 3.2320 ± 0.0003 | 5.1524 ± 0.0008 | 620 ± 88 | 0.05 ± 0.05 | 0.53 ± 0.02 | 0.33 ± 0.02 | 0.14 ± 0.01 |
| 2.1 | 14.91 ± 4.42 | 99.02 ± 0.12<br>0.98 + 0.12 | 3.2378 ± 0.0007 | 5.1449 ± 0.0009 | 563 ± 63 | 0.33 ± 0.03 | 0.58 ± 0.01 | 0.32 ± 0.02 | 0.09 ± 0.01 |
| 2.3 | 23.45 ± 0.63 | 98.26 ± 0.36<br>1.74 + 0.36 | 3.2302 ± 0.0011 | 5.1527 ± 0.0014 | 690 ± 80 | 0.11 ± 0.05 | 0.50 ± 0.04 | 0.37 ± 0.02 | 0.14 ± 0.03 |

presented data, the error of calculating texture *f*-parameters corresponds to the value of the error indicated usually when using the traditional *X*-ray shooting and calculating the Kearns *f*-parameters [20].

### The results of the layer of the inhomogeneity of the studied tubes

Layered inhomogeneity researches were carried out on samples of both alloys No. 1 and No. 2, deformed and annealed at temperatures of 480, 580 and 600 °C for 3 hours. In **Figs. 6–8** the results of changes in the structural characteristics of both alloys are presented: layer-by-layer changes in the volume fraction of the Laves phase in both alloys, the lattice parameter *a*, and changes in microdistortion $\Delta d/d$ with increasing annealing temperature.

**Fig. 6** shows the change in the fraction of the additional Laves phase in alloys of both compositions depending on the annealing temperature of the samples. The graph for the β-phase is not provided, since it is present only in alloy No. 1, the volume fraction of the β-phase in alloy No. 1 does not exceed 0.5% and the lattice parameter changes from 3.31 to 3.62 Å depending on the conditions of thermomechanical treatment, which is described in detail in [9].

**Fig. 7** shows the change in the lattice parameter "*a*" of α-zirconium taking into account the layer-by-layer inhomogeneity of the tubes, which is completely consistent with the results obtained earlier for the same samples using traditional *X*-ray diffraction methods **(Table 1)**. It should be noted that there is a significant spread in the lattice parameter "*a*" across the wall thickness of the tubes, which must be taken into account when preparing samples for *X*-ray and electron microscopic analyses, which are characterized by greater localization over the depth of the studied sample. The layer-by-layer inhomogeneity of the change in the lattice parameter of the deformed tubes indicates increased deformation of the outer layers as a result of rolling compared to the inner layers. Moreover, the degree of deformation of alloy No. 1 is somewhat higher than that of alloy No. 2. This is obvious if we take into account the fact that alloy No. 2 has a higher content of the strengthening intermetallic phase compared to alloy No. 1 (see **Table 2, Fig. 6**).

**Fig. 8** shows how microdistortions are reduced as a result of increasing the annealing temperature of deformed alloys No. 1 and No. 2. Regardless of the amount of the Laves phase in the studied alloys, a monotonic decrease in microdistortions of the crystalline structure of the α-phase is observed with an increase in the annealing temperature of the tubes. Note that annealing at a temperature of 480 °C for 3 hours does not ensure complete annealing of

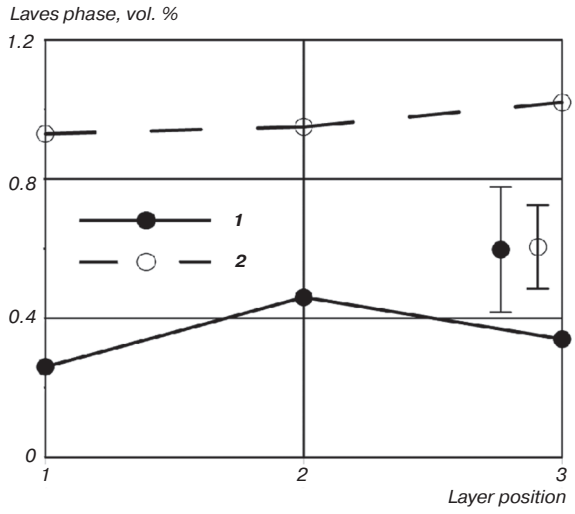


**Fig. 6.** Layer-by-layer change in the volume fraction of the Laves phase in deformed tubes made of the studied alloys No. 1 and No. 2

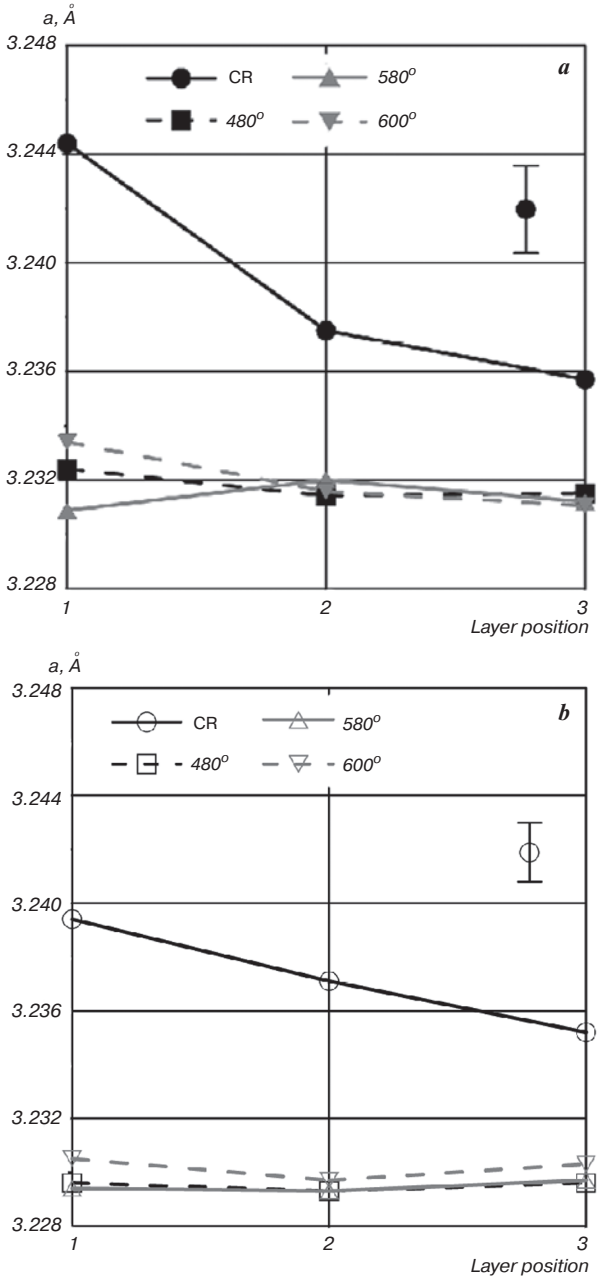


**Fig. 7.** Layer-by-layer change in the lattice parameter in the studied alloys No. 1 (*a*) and No. 2 (*b*)

residual stresses in the product. Annealing at temperatures of 580 and 600 °C for 3 hours helps to eliminate distortions up to 0.1%.

For Russian cladding and channel tubes and, as well as guide channels, it was established [22, 23] that the optimal crystallographic texture is the (0001) ± 30–60° *R-T* <10.0>–<11.0>, for which the texture maximum on the DPF (0001) is deviated from the radial direction by 45° towards the tangential direction, with $f_L$ = 0.1–0.15. This is due to a compromise between properties such as radiation and thermal creep, for which the lowest creep rate is exhibited by CANDU reactor channel tubes with the {11.0}<10.0> texture, and the favorable orientation of hydrides, the habit planes of which are parallel to the basal planes and determine the process of delayed hydride cracking of tubes, i.e. the basal plane should be parallel to the cylindrical surface of the tube. The production of Russian zirconium tubes is aimed at obtaining a high $f_R$-parameter (up to 0.6) and minimal layer-by-layer textural inhomogeneity [2].

Let us consider the obtained results on the crystallographic texture. The rolled tubes are characterized by two stable texture components (0001) ± 30–60° *R-T*<10.0>. **Fig. 9** shows the change in the integral Kearns texture *f*-parameters for three directions in the tube: radial *R*, tangential *T* and axial *L*. With such a texture, the $f_L$-parameter is 0.08-0.13 and determines the rate of radiation growth under irradiation $G \sim (1\text{-}3 f_L)$ [23]. In tubes of both alloys, meridional scattering of the basal axes occurs during recrystallization, which contributes to an increase in the $f_L$-parameters, most clearly observed for the outer layers of the tubes **(Fig. 9)**. In the case of recrystallization of tubes, the $f_L$-parameter for middle layers increases to 0.13. Taking into account the error in the circumferential inhomogeneity of the tubes and the error in reconstructing the ODF from the Debye rings, these changes are insignificant. In this case, the anisotropy of the physical and mechanical properties is determined by the ratio of the $f_R$- and $f_T$-parameters, which depends on the texture maximum position of the basal axes in the *R-T* section of the tubes [22, 23].

In the cold-rolled material, the value of the integral *f*-parameters is determined by the stress state realized in the tube workpiece at the final stage. Since the stable crystallographic texture in the tubes was formed at the previous stages of hot and cold deformation, only a small shift of the texture maxima on the complete DPF (0001) can occur at the final stage, determined by the value of the *Q*-factor in different layers of the tube. The *Q*-factor is the ratio of deformation by the wall thickness and the average diameter of the tube [2, 3]. An increase in the *Q*-factor leads to an increase in the pole density on the complete DPF (0001) near the radial direction. This process is due to the reorientation of the basal normals due to twinning along the planes {10.2} and {11.1} at angles of approximately 85° and 35°, respectively. For both tubes, characterized by different wall thickness (0.6 and 1.0 mm) and

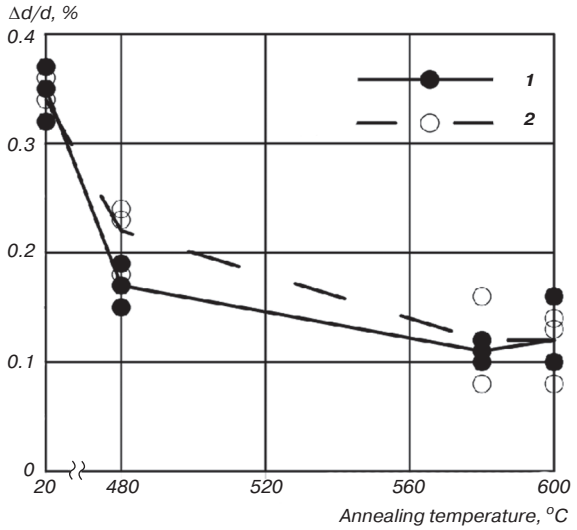


**Fig. 8.** Temperature dependence of microdistortions of the crystal structure of the α-phase in annealed alloys No. 1 and No. 2

various phase composition, an increase in the $f_R$-parameter, a decrease in $f_T$ and the conservation of $f_L$ are observed when moving from the outer layers to the inner ones. This is due to the non-uniformity of the stress state in different layers of the tube during cold rolling.

Annealing of tubes at a temperature of 480 °C corresponds to the polygonization of the material, during which the cold-rolled grains are improved by moving the defects of the crystal structure (point defects, dislocations, disclinations, etc.) to the boundaries of grains or subgrains. During this process, the restoration of the lattice parameters "*a*" and "*c*" is observed, but the half-width of the *X*-ray reflections remains large enough, which indicates the preservation of elastic stresses and explains the change in the microdistortions of the crystal lattice $\Delta d/d$ **(Fig. 8)**. In the case of polygonization, the preferred orientation of the grains is preserved, which is confirmed by the data presented in **Fig. 9**. It is evident that the curves for the cold-rolled and annealed at 480 °C tubes made of alloy No. 1 are located very close, i.e. the differences in the values of the *f*-parameters for the specified tubes do not exceed the measurement error of 0.02, and in alloy No. 2 the curves of the layer-by-layer change in the *f*-parameters for deformed and annealed at 480 °C tubes coincide.

For all recrystallized samples, a meridional broadening of the complete DPF (0001) is observed [2, 9, 10]. Due to the violation of statistics with an increase in grain size, i.e. a decrease in the number of grains participating in diffraction, the main texture maxima on the DPF (0001) with planes (0001) ± 30-45° *R-T* deviated from the *R*-direction towards *T*, are divided into separate maxima corresponding to grains of different orientation. The preferential growth of grains on the slopes of the main texture maxima on the DPF (0001) during recrystallization leads to a blurring of the DPF (0001) in the meridional direction, as was shown in [2, 9, 10], which provides an increase in the integral texture *f*-parameter $f_L$. Note that the greatest increase corresponds to an annealing temperature of 580 °C.

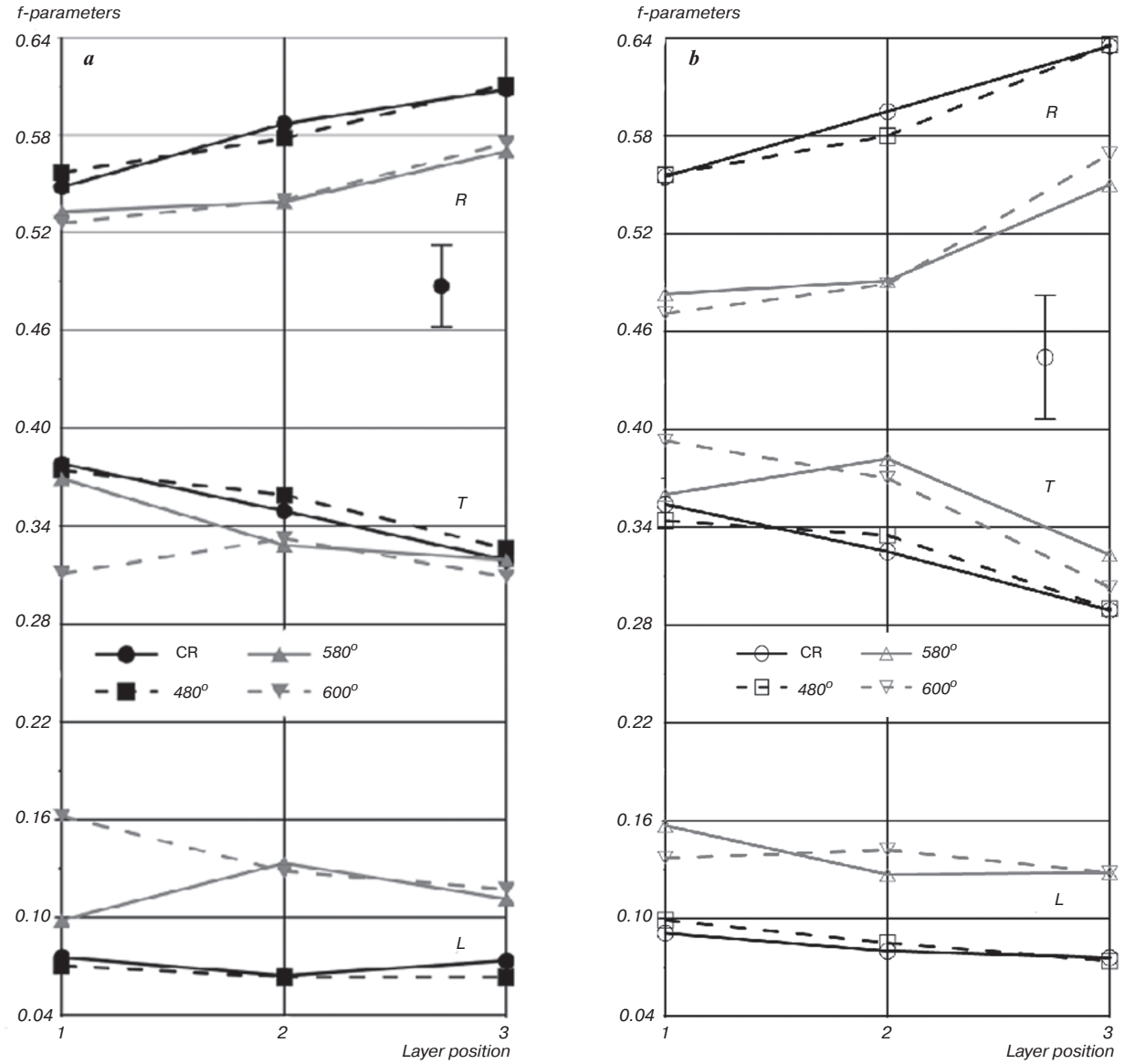


**Fig. 9.** Layer-by-layer change in integral texture *f*-parameters in tubes made of alloys No. 1 (*a*) and No. 2 (*b*) in different states

During recrystallization of zirconium alloys (annealing temperature 560–600 °C), both increase and decrease of $f_R$- and $f_T$-parameters are possible. The direction of texture *f*-parameters change indicates where the texture maxima moved from during the last deformation. This allows us to estimate the *Q*-factor for the last stage of cold rolling. According to the data obtained, the $f_R$-parameter is equalized by the wall thickness of the cladding tube, and the layer-by-layer inhomogeneity in the guide channel tube with a wall thickness of 1 mm is preserved with a general decrease in the value by 0.06, while the $f_T$-parameter increases.

In the production of cladding tubes and guide channels, to obtain optimal performance properties (low rate of thermal and radiation creep, favorable orientation of hydrides, low radiation growth, etc.) at the second-to-last stage of cold rolling, it is possible to use a high value of the *Q*-factor, however, at the final stage of cold deformation, it is necessary to use high degrees of deformation along the wall cross-section and *Q* no more than 1, to prevent the activation of the twinning process, which causes not only the asymmetry of the DPF (0001), as was shown in work [2], but also the reverse reorientation of the basal axes from the radial direction of the twinned volumes of the material to the tangential one during recrystallization.

## Conclusions

1. Using diffraction patterns obtained with synchrotron radiation, a qualitative and quantitative phase analysis of deformed and annealed tubes made of Zr – Nb – (Fe, O) and Zr – Nb – Sn – (Fe, O) alloys was performed. The phases detected in the diffraction patterns confirm the previously known phase composition for the Zr – Nb – (Fe, O) alloy: α-Zr, β-Nb, β-Zr and the Laves phase (intermetallic compound

$Zr(Nb, Fe)_2$; for the Zr – Nb – Sn – (Fe, O) alloy: α-Zr and the Laves phase.

2. An algorithm for studying the crystallographic texture of materials using Debye rings obtained with synchrotron *X*-ray radiation in transmission shooting has been optimized. The grain orientation distribution functions (ODFs) and complete direct pole figures (DPFs) have been calculated for the α-phase of deformed Zr – Nb –(Fe,O) and Zr – Nb – Sn – (Fe,O) alloys, as well as those annealed at different temperatures in the range of 480–600 °C.

3. The efficiency of using synchrotron radiation for studying the layer-by-layer and circumferential inhomogeneity of tubes made of Zr – Nb – (Fe, O) and Zr – Nb – Sn – (Fe, O) alloys is demonstrated in comparison with the labor-intensive procedure of studying the inhomogeneity of tubes using diffractometric shooting of composite samples.

4. The results of circumferential inhomogeneity measurements show that the error in the reconstruction of the ODF depends on the substructural state of the material. Thus, the error in processing the Debye rings obtained for deformed samples is 16–17%, while for annealed samples this error reaches 28%. This is determined by the violation of the statistical significance of the obtained data with grain growth as a result of high-temperature annealing of the studied samples.

5. It was found that in seamless zirconium tubes microstresses are retained in the case of annealing at a temperature of 480 °C, i.e. during polygonization of the material, while the lattice parameters correspond to the recrystallized state.

6. It is shown that in recrystallized cladding tubes made of Zr – 1%Nb alloy, the crystallographic texture of the outer and inner layers differs slightly, i.e., the integral texture *f*-parameters change within the circumferential inhomogeneity of the tubes. While in recrystallized guide channels, characterized by greater wall thickness, these changes are more significant, the differences reaching 0.08.

**Acknowledgements**

***The work was carried out with the financial support of the Russian Science Foundation (project № 24-79-10289, https://rscf.ru/project/24-79-10289/).***

***The authors express their gratitude to the Joint-stock company "Advanced Research Institute of Inorganic Materials named after Academician A. A. Bochvar" for providing samples for the study.***

***X-ray diffraction studies were performed using the unique scientific facility "Kurchatov synchrotron radiation source "KISI-Kurchatov" of the National Research Center "Kurchatov Institute".***

**References**

1. Perlovich Yu. A., Isaenkova M. G. Structural Inhomogeneity of Textured Metallic Materials. Moscow: National Research Nuclear University "MEPhI", 2015. 398 p.

2. Isaenkova M. G., Perlovich Yu. A. Regularities of Crystallographic Texture Development and Substructural Inhomogeneity in Zirconium Alloys During Deformation and Heat Treatment. Moscow: National Research Nuclear University "MEPhI", 2014. 528 p.

3. Kocks U. F., Tomé C. N., Wenk H.-R. Texture and Anisotropy: Preferred Orientations in Polycrystals and Their Effect on Materials Properties. Cambridge University Press, 1998. 676 p.

4. Perlovich Yu., Bunge H. J., Isaenkova M. Inhomogeneous Istribution of Residual Deformation Effects in Textured BCC Metals. *Textures and Microstructures*. 1997. Vol. 29. pp. 241–266.

5. Perlovich Yu., Bunge H. J., Isaenkova M., Fesenko V. The Distribution of Elastic Deformation in Textured Materials as Revealed by Peak Position Figures. *Materials Science Forum*. 1998. Vols. 273-275. pp. 655–666.

6. Isaenkova M. G., Perlovich Yu. A., Soe San Thu, Krymskaya O. A., Fesenko V. A. Development of Crystallographic Texture in the Time of Rolling of Zr Monocrystals and Their Recrystallization. *Tsvetnye Metally*. 2014. No. 12. pp. 73–78.

7. Vishnyakov Ya. D., Babareko A. A., Vladimirov S. A., Egiz I. V. Theory of Texture Formation in Metals and Alloys. Moscow: Nauka, 1979. 343 p.

8. Isaenkova M. G., Petrov M. I., Kozlov I. V., Bogomolova A. V. Structural Features of Hydrogenated E110opt and E635 Tubes. *Non-ferrous Metals*. 2023. No. 1. pp. 41–48.

9. Isaenkova M. G., Krymskaya O. A., Klyukova K. E., Bogomolova A. V., Dzhumaev P. S., Kozlov I. V., Fesenko V. A. Comparison of the Texture Analysis Results of Zirconium Alloys According to the Data of Backscattered Electron Diffraction and *X*-Ray Radiation of Different Power. *Letters on Materials*. 2023. Vol. 13, Iss. 4. pp. 341–346.

10. Isaenkova M., Krymskaya O., Klyukova K., Bogomolova A., Kozlov I., Dzhumaev P., Fesenko V., Svetogorov R. Regularities of Changes in the Structure of Different Phases of Deformed Zirconium Alloys as a Result of Raising the Annealing Temperature According to Texture Analysis Data. *Metals*. 2023. Vol. 13, Iss. 10. 1784.

11. Wenk H.-R., Grigull S. Synchrotron Texture Analysis with Area Detectors. *Journal of Applied Crystallography*. 2003. Vol. 36. pp. 1040–1049.

12. Lutterotti L., Matthies S., Wenk H.-R., Schultz A. S. Richardson J. W. (Jr.). Combined Texture and Structure Analysis of Deformed Limestone from Time-of-Flight Neutron Diffraction Spectra. *Journal of Applied Physics*. 1997. Vol. 81, Iss. 2. pp. 594–600.

13. Lutterotti L., Bortolotti M., Ischia G., Lonardelli I., Wenk H.-R. Rietveld Texture Analysis from Diffraction Images. *Zeitschrift für Kristallographie Supplements*. 2007. Vol. 26. pp. 125–130.

14. Dollase W. A. Correction of Intensities for Preferred Orientation in Powder Diffractometry: Application of the March Model. *Journal of Applied Crystallography*. 1986. Vol. 19. pp. 267–272.

15. Lutterotti L., Vasin R., Wenk H.-R. Rietveld Texture Analysis from Synchrotron Diffraction Images. I. Calibration and Basic Analysis. *Powder Diffraction*. 2014. Vol. 29, Iss. 1. pp. 76–84.

16. Wenk H.-R., Lutterotti L., Kaercher P., Kanitpanyacharoen W., Miyagi L., Vasin R. Rietveld Texture Analysis from Synchrotron Diffraction Images. II. Complex Multiphase Materials and Diamond Anvil Cell Experiments. *Powder Diffraction*. 2014. Vol. 29, Iss. 3. pp. 220–232.

17. Lonardelli I., Wenk H.-R., Lutterotti L., Goodwin M. Texture Analysis from Synchrotron Diffraction Images with the Rietveld Method: Dinosaur Tendon and Salmon Scale. *Journal of Synchrotron Radiation*. 2005. Vol. 12. pp. 354–360.

18. Ischia G., Wenk H.-R., Lutterotti L., Berberich F. Quantitative Rietveld Texture Analysis of Zirconium from Single Synchrotron Diffraction Images. *Journal of Applied Crystallography*. 2005. Vol. 38. pp. 377–380.

19. Lutterotti L. Maud: a Rietveld analysis program designed for the internet and experiment integration. *Acta Crystallographica Section A: Foundations and. Advances*. 2000. Suppll. 56. s54.

20. Kearns J. J. Terminal Solubility and Partitioning of Hydrogen in the Alpha Phase of Zirconium, Zircaloy-2 and Zircaloy-4. *Journal of Nuclear Materials*. 1967. Vol. 22. pp. 292–303.

21. MTEX Software for Analyzing and Modeling Crystallographic Textures by Means of EBSD or Pole Figure Data (TU Chemnitz, Germany). URL: http://mtex-toolbox.github.io (Accessed Date: 26.09.2025).

22. Causey A. R., Woo C. H., Holt R. A. The Effect of Intergranular Stresses on the Texture Dependence of Irradiation Growth in Zirconium Alloys. *Journal of Nuclear Materials*. 1988. Vol. 159. pp. 225–236.

23. Wen W., Capolungo L., Tomé C. N. Mechanism-Based Modeling of Solute Strengthening: Application to Thermal Creep in Zr Alloy. *International Journal of Plasticity*. 2018. Vol. 106, pp. 88–106.

24. Beskorovayny N., Kalin B., Platonov P., Chernov I. Structural Materials of Nuclear Reactors. Moscow: Energoatomizdat, 1995. 704 p.

NFM